

Application of Soft Computing in Forecasting Wave Height (Case Study: Anzali)

Mohammad Akbarinasab¹, Iman Esmaili Paeen Afrakoti^{2*}

¹Assistance Professor, Department of Physical Oceanography, Faculty of Marine Science, University of Mazandaran, Babolsar Mazandaran province, Iran; m.akbarinasab@umz.ac.ir

^{2*} Corresponding author: Assistance Professor, Faculty of Engineering & Technology, University of Mazandaran, Pasdaran Street, Babolsar, Iran; i.esmaili.p@umz.ac.ir

ARTICLE INFO

Article History:

Received: 7 May 2019

Accepted: 16 Jun. 2019

Keywords:

Soft computing techniques
Wave height
Caspian Sea
Prediction

ABSTRACT

Wave height forecasting is very important for coastal management and offshore operations. In this paper, the accuracy and performance of three soft computing techniques [i.e., Multi-Layer Perceptron (MLP), Radial Basis Function Neural Network (RBFNN) and Adaptive Neuro Fuzzy Inference System (ANFIS)] were assessed for predicting significant wave height. Using different combinations of parameters, the prediction was done over a few or a two days' time steps from measured buoy variables in the Caspian Sea (case study: Anzali). The data collection period was from 03.01.2017 to 06.01.2017 with 30-minute intervals. The performance of different models was evaluated with statistical indices such as root mean squared error (RMSE), the fraction of variance unexplained (FVU), and coefficient of determination (R²). Different simulations of performance assessment showed that the ANFIS techniques with requirements of past and current values of atmospheric pressures and height waves has more accuracy than the other techniques in the specified time and location. Meanwhile, in high lead times, the friction velocity decreases the accuracy of wave height forecasting.

1. Introduction

Wave prediction is essential for engineering applications, understanding sediment movement in coastal area and wave energy harvesting. Different approaches have been used for wave height estimating such as Empirical models, Numerical models, and Soft computing techniques. Empirical methods, which are fast and simple, have been developed for primary wave prediction, SMB [1,2], Shore Protection Manual (SPM), Coastal Engineering Manual (CEM) [3], JONSWAP, and SPM [4]. Among the numerical models, we should reference Wave Analysis Model (WAM), which is used primarily for deep-water conditions [5] SWAN that is used mainly for shallow water region [6] etc. Numerical models are generally more accurate than the empirical methods; but, costly and time-consuming [7]. Despite the long history of numerical and empirical models, previous studies have shown that these models have some disadvantages like time-consuming. Implementation of these models requires various parameters such as topography, whitewash, and wind data. Soft computing approaches are introduced as a convenient technique regarding disadvantages of numerical models. Different soft

computing techniques, available to develop wave forecasting models, are Artificial Neural Network (ANN) [8; 9;10;11;12;13;14], Multi-Layer Perceptron (MLP), Radial Basis Function Neural Network (RBFNN), Adaptive Neuro Fuzzy Inference System (ANFIS), Genetic programming, regression trees [15;16], Support Vector Machine (SVM) and etc. Many studies have been carried out to predict wave height using soft computing techniques. The friction velocity (u^*) is one of the most effective parameters in this issue [17; 8]. The main objectives of this article are as follows:

- Comparison of three methods (MLP, RBFNN and ANFIS) of soft computing techniques to predict wave height and choosing the best method for wave height forecasting.
- Investigation various combinations of effective parameters on wave height prediction.

The paper is organized as follows. Section 1, the mentioned three soft computing techniques, MLP, RBFNN, and ANFIS; are used to train models based on the observed data from a wave buoy. In section 2, the observed data are analyzed and a brief definition for the

three soft computing algorithms is represented. In section 3, the study area is defined, combinations of the employed models are mentioned and the models are trained to forecast the wave height in 3 h, 6 h, 12 h, 24 h and 48h based on the observed data. The results of different models are compared in section 4 and finally the discussions of the results are conducted in section 5.

2. Materials and methods

Three different soft computing technologies are used in this study to forecast wave height in the Caspian Sea (Anzali). A brief description of each method is presented as follows.

2.1 Multi-layer perceptron (MLP)

MLP is a kind of artificial neural network which is inspired from human biological brain system. The basic processing element of MLP is called the perceptron neuron which implements a nonlinear type (usually sigmoid) activation function. Each MLP network consists of different layers which are aligned in a feed-forward structure and the data flows in the network through the synaptic weights between neurons. In Figure 1 a general structure of a MLP network is shown.

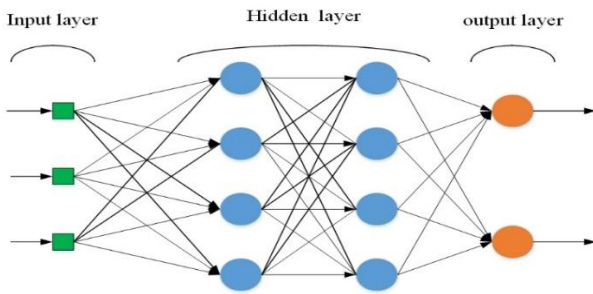


Figure 1. Structure of MLP algorithm

The MLP structure consists of at least 3 layers, input, hidden, and output layer. The input layer receives the value of input variables, hidden layer increase the computation ability of network for non-linear systems and output layer delivers the value of the systems output. MLP is a powerful algorithm in solving a nonlinear supervised problem. The synaptic weights should be computed in the training phase of the algorithm. The back-propagation algorithm is being used for training the network. Applying the training data using back-propagation algorithm the synaptic weights will be set in the training phase, in the modeling phase, applying the test data to the inputs of network will result in the systems output value on the relevant output neuron.

In this paper, 70 percent of data was used for training the network and the other 30 percent was used for testing the algorithm. The network is chosen with three layers, input layer with different number of neurons depends on the chosen model, hidden layer that its

neuron number is chosen with a statistical procedure and output layer with a single neuron.

The transfer function used for the hidden layer is a logarithmic sigmoid function and a pure-line transfer function used for the output node.

2.2 Radial basis function neural network (RBFNN)

2.2.1 Radial basis function

Broomhead and Lowe proposed the RBF neural networks in artificial neural network literature [18]. RBF have shown its efficacy as a soft-computing algorithm in many applications such as function approximation [19], data classification [20], system control [21] and etc.

Input layer, hidden layer and output layer are the main elements of the RBF structure. Input layer receives the inputs of the system to the hidden layer. In the hidden layer a multivariate Gaussian activation function applying to inputs from input layer neurons. The output of the algorithm is being computed based on linear combination of the neurons outputs in hidden layer. The structure of a typical RBN network is shown in Figure 2.

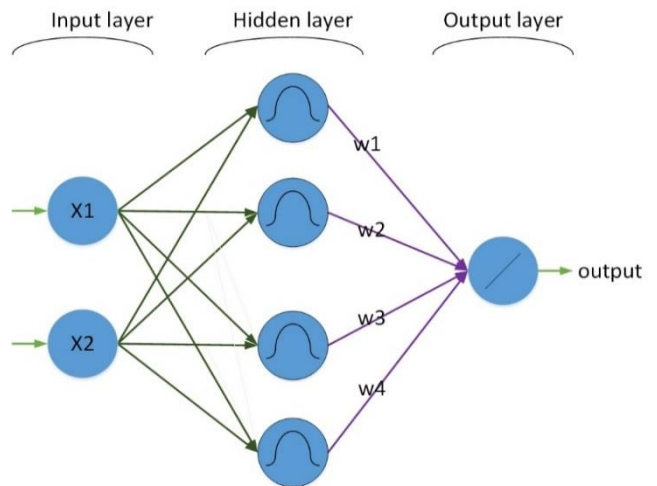


Figure 2. RBF model for a system with two inputs and one output

The RBF model (Figure 2) consists of two input neurons, four Gaussian hidden neurons and a linear neuron as an output neuron which is used for modeling a system with two inputs and one output. The multivariable Gaussian function is used as the activation function for neurons in hidden layer as shown in Equation 1. In Equation (1) the y_j is the output of the j th hidden neuron, \vec{x} is the input vector which is defined as $\vec{x} = [x_1, x_2]$ $\vec{\mu}_j$ is the center of j th hidden neuron which is defined by $\vec{\mu}_j = [\mu_{1j}, \mu_{2j}]$ and σ_j is the variance of the Gaussian function and assumed equal for both x_1 and x_2 variables.

$$y_j = \exp\left(\frac{-\|\vec{x} - \vec{\mu}_j\|^2}{\sigma_j^2}\right) \tag{1}$$

After computation the activation of each hidden neuron, their output will be feed to the output neuron and its output can be defined by linear combination of the all hidden neurons output as shown in Equation (2).

$$y_{out} = \sum_j w_j y_j = \sum_j w_j \exp\left(-\frac{\|\bar{x} - \bar{\mu}_j\|^2}{\sigma_j^2}\right) \quad (2)$$

One or more Gaussian function may be activated by an input vector, because depend on their centers and variances the Gaussian may have overlap with each other, So linear combination of the activated receptive fields (Gaussian functions in RBF network) will be used for computation of models output.

Many parameters in RBF structure such as number of neurons in hidden layer, center and variance of Gaussian functions and the w_j coefficients are existed which should be defined by a suitable learning algorithm. The number of neurons in the hidden layer in many applications is set to the number of training sample, and each training sample will be the center of a Gaussian function and all the variances are set to a fixed value. The w_j coefficients can be defined by minimizing the error function as shown in Equation 3, which y_{ii} is the real output of the i th training sample and y_{mi} is the output of the constructed model. Minimization of this error function can be done by any suitable optimization algorithm like gradient decent [22], genetic algorithm [23] and etc.

$$Error = \sum_{i=1}^n \|y_{ii} - y_{mi}\|^2 \quad (3)$$

In this paper all the simulations have been conducted in MATLAB environment using its RBF toolbox.

2.3 Adaptive Neuro Fuzzy Inference System (ANFIS)

The main concept of using the advantages of both fuzzy inference and artificial neural network algorithm was the reason of developing the ANFIS algorithm in early 1990 by Jang [22]. The effectiveness of the proposed ANFIS algorithm has been shown in different engineering applications such as modeling, control, classification and etc. [25; 26; 27; 29]. ANFIS algorithm is shown to be a universal approximate [29]. The structure of ANFIS algorithm consists of five layers is shown in Figure 3. Responsibility of each layer will be discussed as follows with more details:

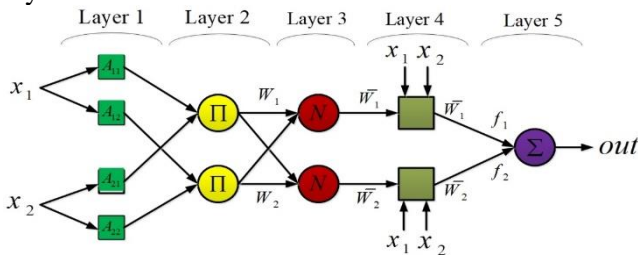


Figure 3. Structure of ANFIS algorithm

Layer1:

Each node in this layer consists of a membership function A_{ij} . The input of each node in this layer is x_i (one of system input) and output is a number between 0 and 1 that shows the degree which x_i satisfies A_k . A_i is a linguistic variable like small, big and etc.

Layer2:

The output node in this layer is the product of their inputs, for example $w_1 = A_{11}(x_1) \times A_{21}(x_2)$, and actually, the output of these nodes can be the application of any T-norm operators that perform generalized AND can be used as a node function.

Layer3:

The output node in this layer is ratio of corresponding w_i to the sum of all w_k : $k=1: n$.

$$\bar{w}_1 = \frac{w_1}{w_1 + w_2}$$

Layer4:

The output nodes in this layer will be as follows:

$$o_i = \bar{w}_i \times f_i = \bar{w}_i \times (p_i x_1 + q_i x_2 + r_i)$$

where, \bar{w}_i is the output of the previous layer and $\{p_i, q_i, r_i\}$ are the parameter set which should be computed in learning mechanism.

Layer5:

The single node in this layer, computes the overall output of the system as follow:

$$out = f(x_1, x_2) = \sum_i \bar{w}_i \times f_i$$

Computation of the parameters can be done by various learning algorithms such as gradient descent, evolutionary algorithms and etc. For learning phase, a suitable error measure should be selected; thus the learning algorithm should select the parameters for minimizing the error.

In this paper, the `genfis3` function of MATLAB is used for implementation of the ANFIS algorithm.

2.4 Statistical criteria

Since the variation of input parameters is not homogeneous, therefore, according to Equation 4, the data were normalized

$$x_{normal} = \frac{x - \bar{x}}{\sigma} \quad (4)$$

where x , \bar{x} and σ are the measurement, mean and variance values of observed data respectively. Normalized data is applied to different algorithms. The output wave height of the model by the inverse process of the Equation (4) is returned to its original state.

In this study, three statistical criteria, namely, The correlation coefficient, R, the mean square error RMSE and fraction of variance unexplained (FVU) were used for evaluating of different models and algorithms.

Correlation coefficient, R, was used as:

$$R = \frac{\sum_i ((x_i - \bar{x}) \times (y_i - \bar{y}))}{\sqrt{\sum_i (x_i - \bar{x})^2 \sum_i (y_i - \bar{y})^2}} \quad (5)$$

In order to evaluate the spread of the predicted values, RMSE, can be defined as:

$$MSE = \sqrt{\frac{\sum_i (x_i - y_i)^2}{n}} \quad (6)$$

In order to evaluate the fraction of variance unexplained, FVU can be defined as:

$$FVU = \frac{VAR_{err}}{VAR_{tot}} = \frac{\frac{SS_{err}}{n}}{\frac{SS_{tot}}{n}} = \frac{SS_{err}}{SS_{tot}}$$

$$SS_{err} = \sum_{i=1}^N (x_i - y_i)^2 \quad (7)$$

$$SS_{tot} = \sum_{i=1}^N (x_i - \bar{x})^2$$

where, xi and yi represent the observed and predicted values at ith time step, respectively, \bar{x} is the mean of observed values, and N is the number of observations.

2.5 Observed data

Wave data collected by a buoy deployed at 15 meter depth at 49°53'0"E and 37°25'0"N off the Anzali coast (south of the Caspian Sea). Data collection was done by I.R. Iran Meteorological Organization (IRIMO). The data cover the period from 03.01.2017 to 06.01.2017 with 30-minute intervals. The statistic of recorded data is provided in Table 1.

Figure 5 shows the wind rose diagram of observed data. As can be seen, winds are predominantly from east.

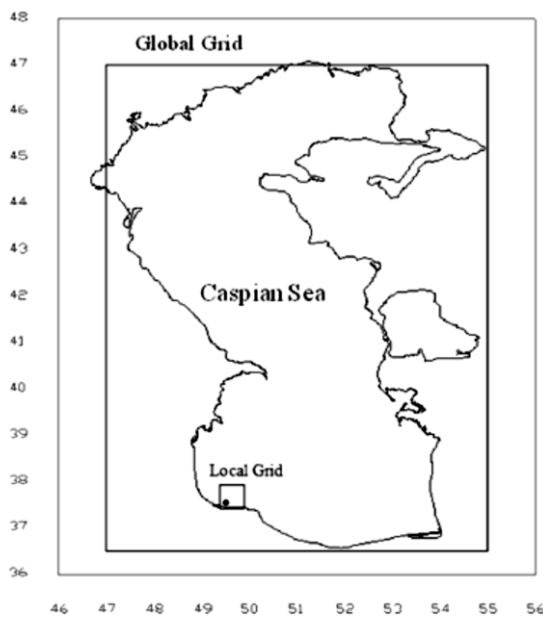


Figure 4. Map of the Caspian Sea and location of the buoy.

Table 1. Statistics of recorded data

Parameter	Minimum	Maximum	Average
Atmospheric pressure (hPa)	999.28	1035.95	1016.5
Wave height (m)	0.06	1.71	0.3556
Wave period (s)	1.4	4.5	2.409
Wind direction (deg)	0	359.69	145.69
Wind speed (m/s)	0	9.71	2.28
Current direction (deg)	0	359.69	169.31
Current surface(cm/s)	0.29	72.74	16.06

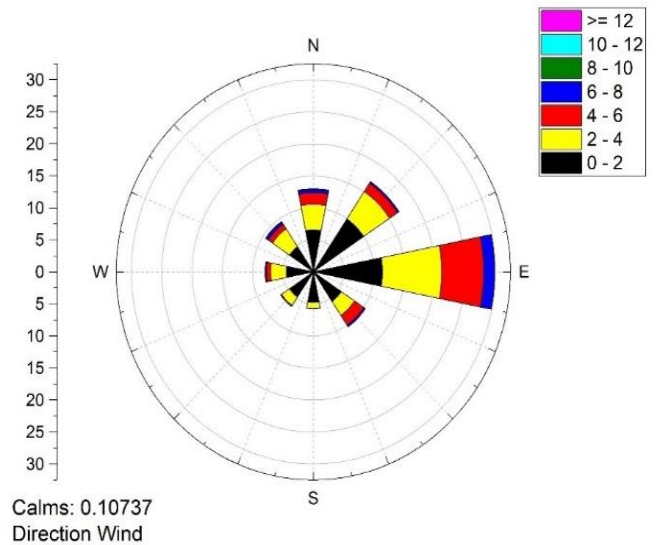


Figure 5. Wind rose diagram for study period of Anzali

The time series in Figure 6 shows the wave height, atmospheric pressure, and wind speed during the study period.

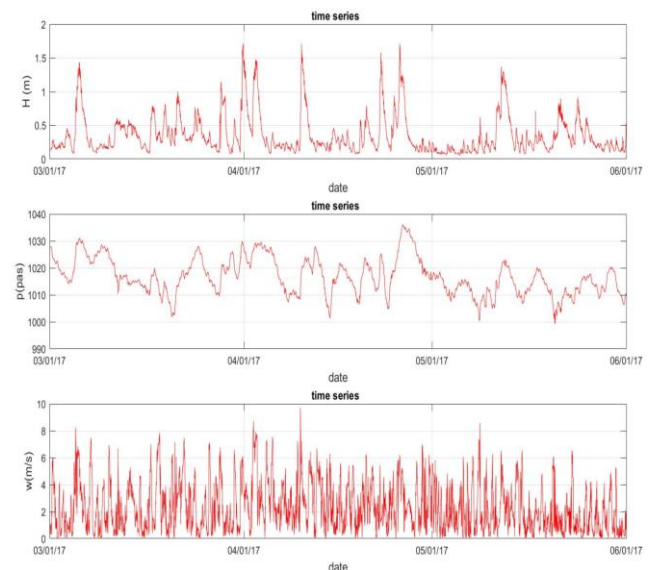


Figure 6. Half-hourly variations of the used training and testing data sets: (a) wave height (b) atmospheric pressure (c) wind speed during (01.03.2017 to 01.06.2017) in Anzali.

2.6 The models

Accurate prediction of wave height needs identification of influence factors on wave generation. One of the important factors in forecasting wave parameters is wind speed. Earlier studies showed that using shear velocity, U^* , instead of wind speed at 10m height increases the accuracy of the model in the extreme events [30; 31; 32].

According to Deo et al [33] sensitivity study showed that consideration of fetch and duration neither helps in achieving training nor in improving accuracy of the output.

In this study, in addition to accepting the suggestions of the previous studies, the atmospheric pressure parameter was applied to predict the wave in some models. For the analysis and predication, friction velocity, atmospheric pressure, wave height and wave period at current time and previous time were entered into the models and algorithms to predict significant wave height in different lead times (3h, 6h, 12h, 24h and 48h).

In this paper, the following models were used to predict wave height.

Model A:

$$H_{t+i} = f(H_t, H_{t-1}, H_{t-2}, P_t, P_{t-1}, P_{t-2}, \dots, P_{t-7})$$

Model B:

$$H_{t+i} = f(H_t, H_{t-1}, H_{t-2}, U_t^*, U_{t-1}^*, U_{t-2}^*, \dots, U_{t-7}^*)$$

Model C:

$$H_{t+i} = f(H_t, H_{t-1}, H_{t-2}, U_t^* \cos(\varphi_t - \theta_t), U_{t-1}^* \cos(\varphi_{t-1} - \theta_t), U_{t-2}^* \cos(\varphi_{t-2} - \theta_t))$$

ModelD:

$$H_{t+i} = f(H_t, H_{t-1}, H_{t-2}, P_t, P_{t-1}, P_{t-2})$$

where, “i” indicates the forecasting lead time of 3, 6, 12, 24, and 48h.

In these models, the variables include significant wave height (H_t), sea surface wind speed (U), wave direction (θ_t), wind direction (φ_t), pressure air (P).

In order to select the best number of neurons in hidden layer, the models were run with different number of neurons. Then, based on the root mean squared error (RMSE) and coefficient of determination (R), the best number of neuron was determined for each model. Figure 7 shows a typical process of determining the neurons number.

The results of selecting the best number of neurons in the hidden layer for all of prediction lead-time are shown in Table 2.

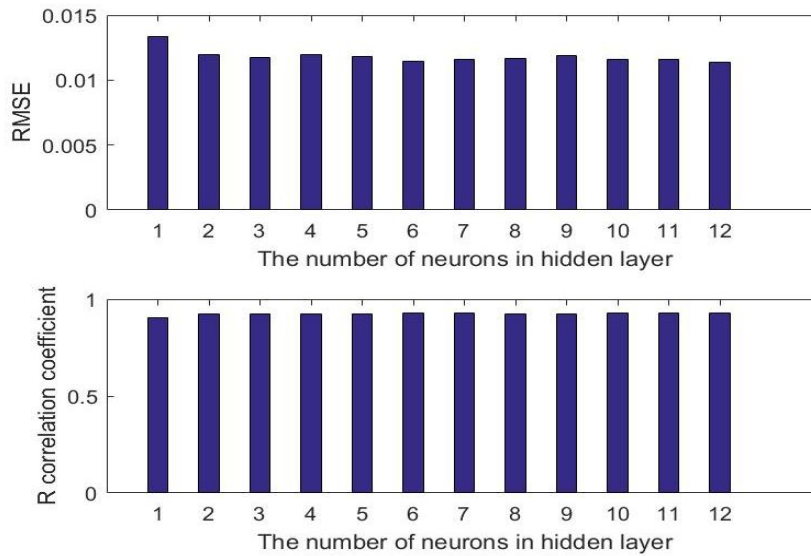


Figure 7. Assessment of the number of neurons in the hidden layer

Table 2. The best number of hidden layer neurons of each model to forecast lead-time in MLP algorithm.

	lead time(h)	3	6	12	24	48
model A	The correlation coefficient (R)	0.9273	0.83	0.66	0.39	0.33
	MLP_std_reg	0.01138	0.0241	0.045	0.069	0.072
	Number of neurons in the hidden layer	10	5	11	12	11
Model B	The correlation coefficient (R)	0.9211	0.8089	0.55	0.219	0.12
	MLP_std_reg	0.012	0.02841	0.056	0.077	0.081
	Number of neurons in the hidden layer	4	5	3	7	5
Model C	The correlation coefficient (R)	0.92	0.8	0.547	0.22	0.069
	MLP_std_reg	0.0122	0.029	0.5695	0.077	0.081
	Number of neurons in the hidden layer	2	2	10	6	10
Model D	The correlation coefficient (R)	0.928	0.833	0.65	0.3968	0.37
	MLP_std_reg	0.011	0.0249	0.0469	0.068	0.071
	Number of neurons in the hidden layer	11	12	12	7	12

3. Results and Discussion

The present study aims at the application of MLP, RBF, and ANFIS to carry out the real-time forecasting of significant wave heights over time steps of a few or two days at a specified location and season. Tables 3 to 6 show the error statistics in the testing stages of three algorithms for the models A, B, C, and D. As shown, when the model B (the model without atmospheric

pressure inputs) is compared with the models A and D (the model without friction velocity inputs). The results of models B and C have less accuracy than those of models A and D in large lead-time. This means that the need for atmospheric pressure parameters as inputs is very important in long-time forecasting. The bold numbers in tables 3 to 6 show output better than other algorithms.

Table 3. Error indices for all three algorithms in model A for 3- 48 hourly forecasting times

	lead times(h)	Algorithm	FVU_error	std_FVU	RMSE_error	std_mse	R_coef	std_reg
Model A	3	MLP	0.228	0.027	0.096	0.004	0.914	0.009
	3	RBF	0.222	0.014	0.094	0.003	0.919	0.005
	3	ANFIS	0.163	0.000	0.007	0.000	0.931	0.000
	6	MLP	0.614	0.078	0.133	0.005	0.825	0.016
	6	RBF	0.729	0.060	0.141	0.005	0.803	0.016
	6	ANFIS	0.455	0.000	0.016	0.000	0.845	0.000
	12	MLP	2.042	0.429	0.195	0.017	0.553	0.107
	12	RBF	2.939	0.242	0.187	0.008	0.617	0.056
	12	ANFIS	1.575	0.000	0.029	0.000	0.697	0.000
	24	MLP	7.344	1.668	0.261	0.003	0.106	0.044
	24	RBF	15.194	0.991	0.224	0.006	0.453	0.114
	24	ANFIS	11.572	0.000	0.047	0.000	0.555	0.000
	48	MLP	5.251	1.644	0.262	0.013	0.106	0.071
	48	RBF	6.558	0.927	0.252	0.005	0.149	0.010
	48	ANFIS	20.796	0.000	0.055	0.000	0.308	0.000

Table 4. Error indices for all three algorithms in model B for 3 to 48 hourly forecasting times

	lead times	Algorithm	FVU_error	std_FVU	RMSE_error	std_mse	R_coef	std_reg
Model B	3	MLP	0.189	0.028	0.088	0.005	0.927	0.008
	3	RBF	0.204	0.003	0.091	0.000	0.922	0.001
	3	ANFIS	0.164	0.000	0.007	0.000	0.930	0.000
	6	MLP	0.560	0.081	0.131	0.004	0.833	0.011
	6	RBF	0.671	0.014	0.139	0.001	0.808	0.002
	6	ANFIS	0.498	0.000	0.017	0.000	0.834	0.000
	12	MLP	3.025	0.781	0.186	0.007	0.622	0.033
	12	RBF	3.252	0.018	0.190	0.000	0.596	0.000
	12	ANFIS	2.272	0.000	0.032	0.000	0.656	0.000
	24	MLP	24.234	12.545	0.232	0.005	0.200	0.072
	24	RBF	27.049	3.888	0.227	0.004	0.278	0.079
	24	ANFIS	39.890	0.000	0.050	0.000	0.405	0.000
	48	MLP	19.123	5.399	0.251	0.004	-0.117	0.030
	48	RBF	15.844	0.316	0.253	0.001	-0.111	0.015
	48	ANFIS	34.660	0.000	0.059	0.000	-0.052	0.000

Table 5. Error indices for all three algorithms in model C for 3 to 48 hourly forecasting times

	lead times	Algorithm	FVU_error	std_FVU	RMSE_error	std_mse	R_coef	std_reg
Model C	3	MLP	0.162	0.005	0.087	0.001	0.927	0.001
	3	RBF	0.170	0.002	0.087	0.000	0.927	0.000
	3	ANFIS	0.167	0.000	0.008	0.000	0.928	0.000
	6	MLP	0.479	0.041	0.130	0.001	0.831	0.003
	6	RBF	0.507	0.002	0.132	0.001	0.825	0.002
	6	ANFIS	0.499	0.000	0.017	0.000	0.834	0.000
	12	MLP	2.635	0.185	0.185	0.001	0.623	0.009
	12	RBF	2.449	0.113	0.182	0.001	0.643	0.002
	12	ANFIS	2.258	0.000	0.032	0.000	0.660	0.000
	24	MLP	19.982	8.050	0.222	0.003	0.359	0.036
	24	RBF	17.107	0.700	0.222	0.002	0.366	0.036
	24	ANFIS	42.402	0.000	0.050	0.000	0.405	0.000
	48	MLP	83.165	75.203	0.241	0.003	-0.069	0.037
	48	RBF	29.049	3.053	0.244	0.001	-0.066	0.004
	48	ANFIS	86.229	0.000	0.057	0.000	-0.074	0.000

Table 6. Error indices for all three algorithms in model D for 3- 48 hourly forecasting times

	lead times	Algorithm	FVU_error	std_FVU	RMSE_error	std_mse	R_coef	std_reg
Model D	3	MLP	0.221	0.041	0.096	0.008	0.913	0.016
	3	RBF	0.197	0.011	0.089	0.002	0.927	0.003
	3	ANFIS	0.164	0.000	0.007	0.000	0.931	0.000
	6	MLP	0.800	0.150	0.152	0.013	0.761	0.051
	6	RBF	0.725	0.086	0.140	0.007	0.807	0.022
	6	ANFIS	0.483	0.000	0.016	0.000	0.839	0.000
	12	MLP	2.879	1.191	0.196	0.015	0.539	0.107
	12	RBF	3.145	0.198	0.187	0.009	0.625	0.076
	12	ANFIS	1.712	0.000	0.030	0.000	0.680	0.000
	24	MLP	8.403	6.649	0.251	0.008	0.162	0.062
	24	RBF	14.249	0.799	0.230	0.002	0.388	0.070
	24	ANFIS	10.555	0.000	0.048	0.000	0.530	0.000
	48	MLP	2.944	0.953	0.313	0.043	0.035	0.078
	48	RBF	5.464	0.874	0.255	0.004	0.147	0.002
	48	ANFIS	18.118	0.000	0.055	0.000	0.309	0.000

Figure 8 shows scatter plots for all the considered models. This plot displays the direct Comparison between the observed and forecasted H computed by three algorithms for model A in different lead-times: (a) 3h, (b) 6h. (c)12h, and (d) 24h. For short lead times (3h and 6 h), the data are dense around the first quadrant bisector, but for large lead times (24h), the

performance of all methods were reasonable in the small wave height. So For the lead time of 24 h, the prediction accuracy further dropped down. The correlation coefficient of all three methods for 3 h lead time is in the same range (0.927–0.93); however, by increasing the lead time, the correlation coefficient of all methods decreases

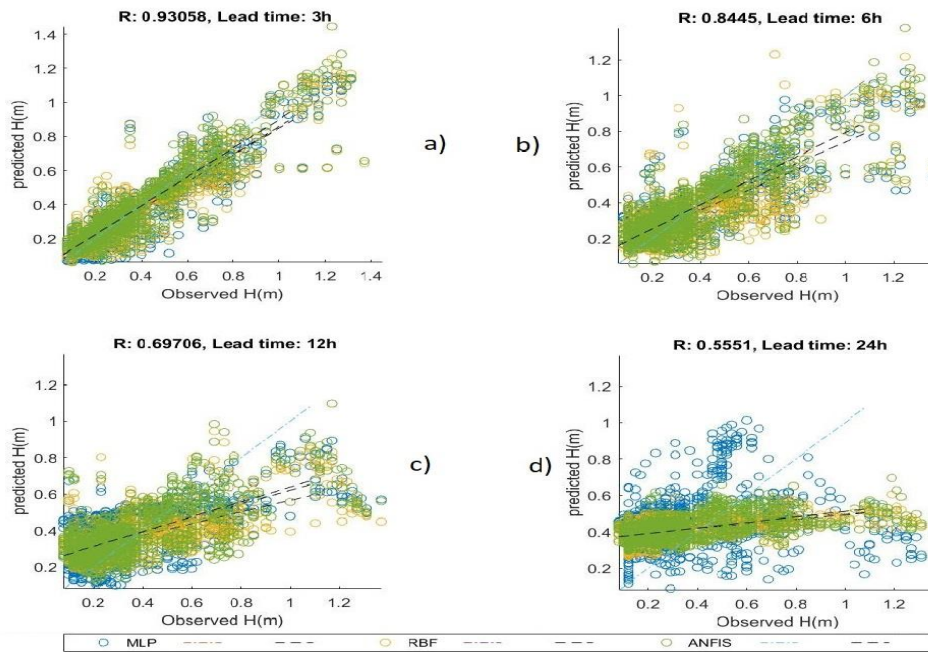
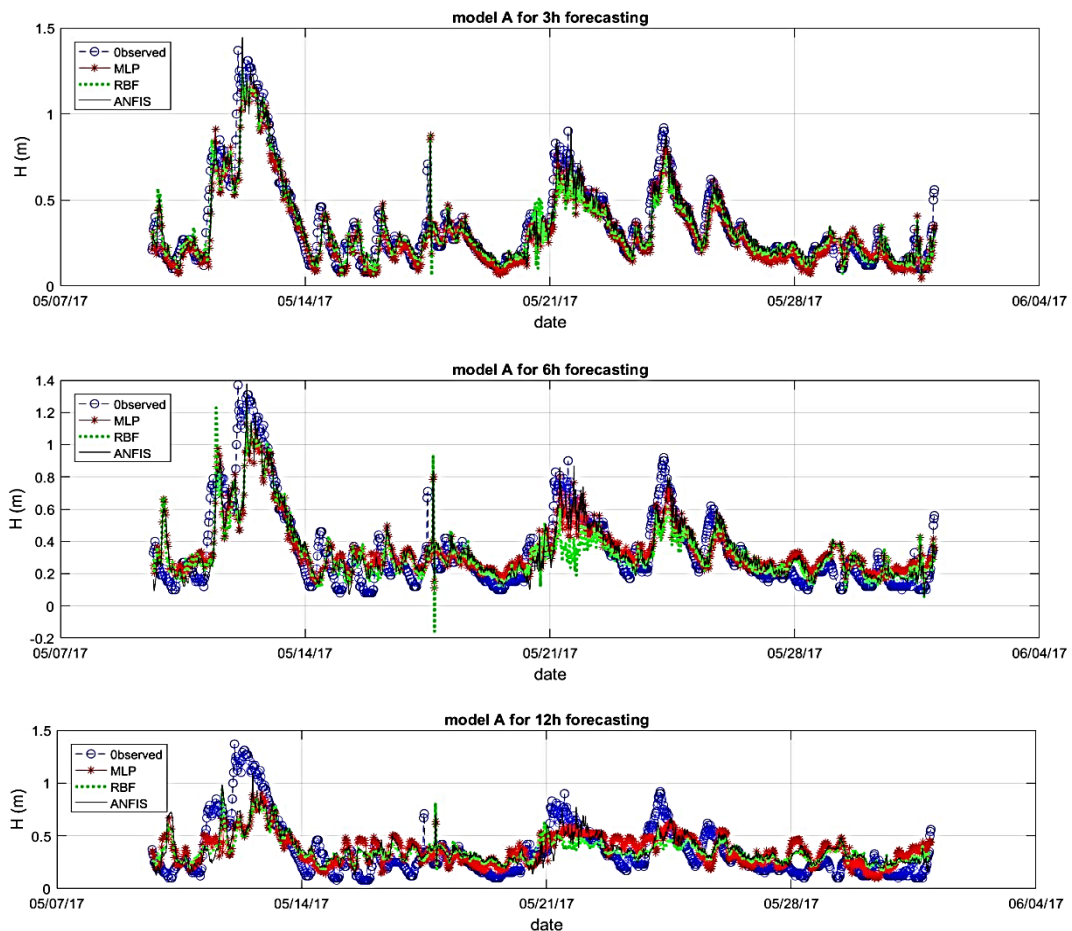


Figure 8. Comparison between the observed and forecasted H computed by three algorithm for model A and different lead-time: (a) 3h, (b) 6h, (c) 12h, and (d) 24h

Figure 9 shows the observed and predicted wave height computed by different algorithms during the analysis 05.12.2017 to 06.01.0217 for model A in 3, 6, 12, 24, and 48h lead times. Fig. 9a shows the forecast for short lead time (3 h) where all three algorithms were well

trained and able to forecast almost whole time period including one hurricane. For 6 h lead time (Fig. 9b), 12h (Fig. 9c), 24 h (Fig. 9d) and 48 h (Fig. 9e), ANFIS algorithm was well trained to forecast of significant height.



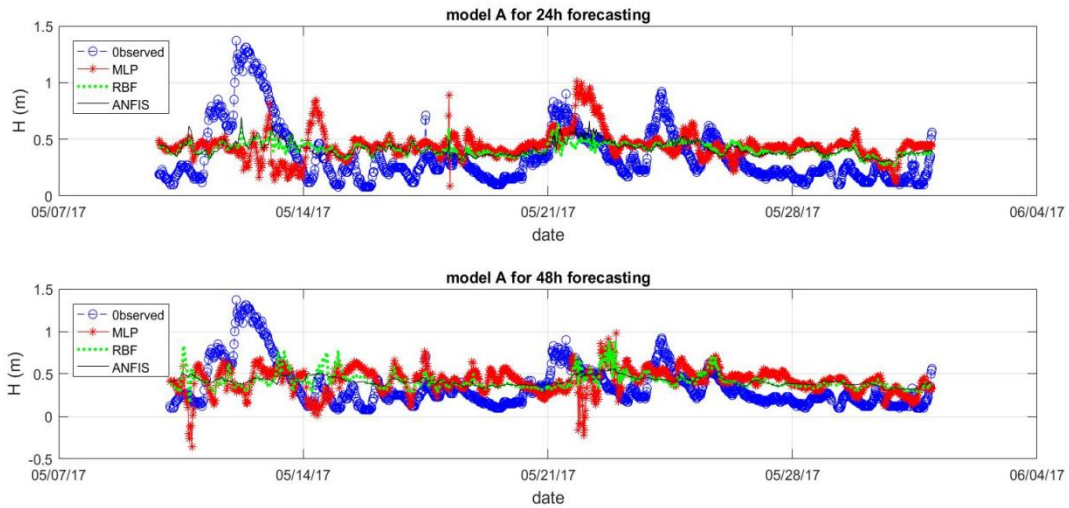


Figure 9. Predicted and observed wave height during test period using three methods and different lead-times: (a) 3h, (b) 6h, (c) 12h, (d) 24h (e) 48h

4. Conclusion

This research mainly focused on predicting significant wave height over the Caspian Sea (Anzali) for winter season by different soft computing methods; Multi-layer perceptron (MLP), radial basis function neural network (RBFNN) and Adaptive Neuro Fuzzy Inference System (ANFIS). In order to investigate the effectiveness of each parameter, all four-mentioned model were applied to three soft computing techniques (MLP, RBF and ANFIS) with normalized input and output. The results showed that using atmospheric pressure instead of friction velocity and significant wave height at current time, $H_{h,s}$, $H_{h,s-1}$, and $H_{h,s-2}$ increases the accuracy of the model in short and long lead times based on ANFIS algorithm. Meanwhile, in any combination that contains the atmospheric pressure parameter, the results indicated a higher accuracy. Also, in long lead times, the predicted wave height does not correlate to the pervious and current friction velocity. In summary, Figure 10 shows the comparison of error indices of the models for different lead-times by ANFIS algorithm. As the figure indicates, the model A has better results than other models.

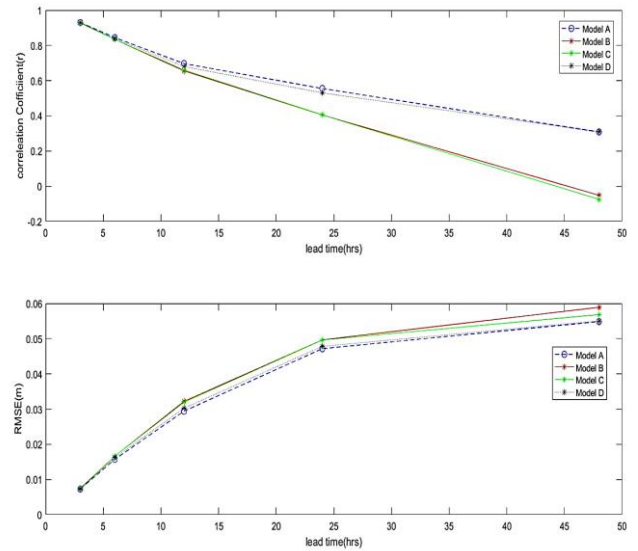


Figure 10. Comparison of error indices in different methods for different lead-times; (a) Variations of correlation coefficient (R) (b) RMSE, vs. forecasting lead-time

References

- 1- Bretschneider, C. L., (1951). *Revised wave forecasting relationships*. Coastal Engineering Proceedings, 1(2), 1.
- 2-Sverdrup, H. U., & Munk, W. H.,(1947), *Wind, sea, and swell: theory of relations for forecasting*.
- 3-Army, U. S., (2003), *Coastal engineering manual, chapter II-2, meteorology and wave climate*. US Army Engineer Waterways Experiment Station, US Government Printing Office, No. EM, 1110–1112.
- 4- Donelan, M. A., (1980). *Similarity theory applied to the forecasting of wave heights, periods and directions*. National Water Research Institute.
- 5- Booij, N., Ris, R. C., and Holthuijsen, L. H., (1999), *A third- generation wave model for coastal regions: 1. Model description and validation*. Journal of Geophysical Research: Oceans, 104(C4), 7649–7666.
- 6- Komen, G. J., Cavaleri, L., and Donelan, M., (1996), *Dynamics and modelling of ocean waves*. Cambridge university press.

- 7- Goda, Y., (2003), *Revisiting Wilson's formulas for simplified wind-wave prediction*. Journal of Waterway, Port, Coastal, and Ocean Engineering, 129(2), 93–95.
- 8- Mahjoobi, J., Etemad-Shahidi, A., and Kazeminezhad, M. H., (2008), *Hindcasting of wave parameters using different soft computing methods*. Applied Ocean Research, 30(1), 28–36.
- 9- Makarynsky, O., (2004), *Improving wave predictions with artificial neural networks*. Ocean Engineering, 31(5–6), 709–724.
- 10- Tsai, C.-P., & Lee, T.-L., (1999), *Back-propagation neural network in tidal-level forecasting*. Journal of Waterway, Port, Coastal, and Ocean Engineering, 125(4), 195–202.
- 11- Vimala, J., Latha, G., and Venkatesan, R., (2014). *Real time wave forecasting using artificial neural network with varying input parameter*.
- 12- Dezvareh, R., (2019). *Application of Soft Computing in the Design and Optimization of Tuned Liquid Column–Gas Damper for Use in Offshore Wind Turbines*. International Journal of Coastal and Offshore Engineering, 2(4), pp.47-57.
- 13- Dezvareh, R., (2019). *Providing a new approach for estimation of wave set-up in Iran coasts*. Research in marine sciences, 4(1), 438-448.
- 14- Dezvareh, R., Bargi, K. and Moradi, Y., (2012). *Assessment of Wave Diffraction behind the Breakwater Using Mild Slope and Boussinesq Theories*. International Journal of Computer Applications in Engineering Sciences, 2(2).
- 15- Etemad-Shahidi, A., and Mahjoobi, J., (2009), *Comparison between M5' model tree and neural networks for prediction of significant wave height in Lake Superior*. Ocean Engineering, 36(15–16), 1175–1181.
- 16- Samadi, M., Jabbari, E., and Azamathulla, H. M., (2014), *Assessment of M5' model tree and classification and regression trees for prediction of scour depth below free overfall spillways*. Neural Computing and Applications, 24(2), 357–366.
- 17- Kazeminezhad, M. H., Etemad-Shahidi, A., & Mousavi, S. J., (2005), *Application of fuzzy inference system in the prediction of wave parameters*. Ocean Engineering, 32(14–15), 1709–1725.
- 18- Broomhead, D. S., and Lowe, D., (1988), *Radial basis functions, multi-variable functional interpolation and adaptive networks*. Royal Signals and Radar Establishment Malvern (United Kingdom).
- 19- Powell, M. J. D., (1985), *Radial basis function for multivariable interpolation: a review*. In IMA Conference on Algorithms for the Approximation of Functions and Data, 1985. RMCS.
- 20- Belloir, F., Fache, A., and Billat, A., (1999), *A general approach to construct RBF net-based classifier*. In ESANN (pp. 399–404). Citeseer.
- 21- Li, Y., Qiang, S., Zhuang, X., and Kaynak, O., (2004), *Robust and adaptive backstepping control for nonlinear systems using RBF neural networks*. IEEE Transactions on Neural Networks, 15(3), 693–701.
- 22- Karayiannis, N. B., (1999), *Reformulated radial basis neural networks trained by gradient descent*. IEEE Transactions on Neural Networks, 10(3), 657–671.
- 23- Chen, S., Wu, Y., and Luk, B. L., (1999), *Combined genetic algorithm optimization and regularized orthogonal least squares learning for radial basis function networks*. IEEE Transactions on Neural Networks, 10(5), 1239–1243.
- 24- Jang, J.-S., (1993), *ANFIS: adaptive-network-based fuzzy inference system*. IEEE Transactions on Systems, Man, and Cybernetics, 23(3), 665–685.
- 25- Manoj, S. B. A., (2011), *Identification and control of nonlinear systems using soft computing techniques*. International Journal of Modeling and Optimization, 1(1), 24.
- 26- Pradhan, B., (2013), *A comparative study on the predictive ability of the decision tree, support vector machine and neuro-fuzzy models in landslide susceptibility mapping using GIS*. Computers & Geosciences, 51, 350–365.
- 27- Tushar, A., & Pillai, G. N., (2015), *Extreme Learning ANFIS for classification problems*. In Next Generation Computing Technologies (NGCT), 1st International Conference on (pp. 784–787). IEEE.
- 28- Kaplan, K., Kuncan, M., and Ertunc, H. M., (2015), *Prediction of bearing fault size by using model of adaptive neuro-fuzzy inference system*. In Signal Processing and Communications Applications Conference (SIU), pp. 1925–1928. IEEE.
- 29- Jang, J.-S. R., Sun, C.-T., and Mizutani, E. (1997), *Neuro-fuzzy and soft computing; a computational approach to learning and machine intelligence*.
- 30- Zamani, A., Solomatine, D., Azimian, A., and Heemink, A., (2008), *Learning from data for wind-wave forecasting*. Ocean Engineering, 35(10), 953–962.
- 31- Kamranzad, B., Etemad-Shahidi, A., and Kazeminezhad, M. H. (2011), *Wave height forecasting in Dayyer, the Persian Gulf*. Ocean Engineering, 38(1), 248–255.
- 32- Mafi, S., and Amirinia, G., (2017), *Forecasting hurricane wave height in Gulf of Mexico using soft computing methods*. Ocean Engineering, 146, 352–362.
- 33- Deo, M. C., Jha, A., Chaphekar, A. S., and Ravikant, K. (2001). *Neural networks for wave forecasting*. Ocean Engineering, 28(7), 889-898.